Dyes and Pigments 93 (2012) 1463–1470

Contents lists available at SciVerse ScienceDirect

Dyes and Pigments

journal homepage: www.elsevier.com/locate/dyepig

The synthesis, photophysical and thermal properties of novel 7-hydroxy-4-methylcoumarin tetrasubstituted metallophthalocyanines with axial chloride ligand

Jun-Jie Guo [a,b], Shi-Rong Wang [a,*], Xiang-Gao Li [a], Ming-Yue Yuan [c]

[a] School of Chemical Engineering, Tianjin University, 300072 Tianjin, China
[b] School of Science, Tianjin University of Commerce, 300134 Tianjin, China
[c] College of Science, Agricultural University of Hebei, 071001 Baoding, China

ARTICLE INFO

Article history:
Received 3 August 2011
Received in revised form
6 October 2011
Accepted 7 October 2011
Available online 25 October 2011

Keywords:
Phthalocyanines
Fluorescence quantum yields
Fluorescence lifetime
Thermal stability
Axial coordination
7-Hydroxy-4-methylcoumarin

ABSTRACT

This work reports the synthesis of 7-hydroxy-4-methylcoumarin tetrasubstituted Ruthenium (III)(**4a**), Indium (III)(**4b**), Tin (IV)(**4c**) phthalocyanines bearing axial chloride ligand for the first time. These new metallophthalocyanines show good solubility in many organic solvents. This study also investigates the photophysical (fluorescence quantum yield and lifetime) properties of compounds **4a**, **4b** and **4c**. The fluorescence of these three metallophthalocyanines is effectively quenched by the addition of 1,4-benzoquinone (BQ). The thermal stability studies indicate that both **4a** and **4b** are stable up to 300 °C.

1. Introduction

Phthalocyanines are important blue and green 18-π electron macrocyclic conjugated compounds which play a major role in modern technology with application in many fields such as semiconductor devices [1], photodynamic therapy [2–4], organic light-emitting devices [5], sensors [6], non-linear optics [7], and photovoltaic solar cells [8–10]. They have high chemical and thermal stability and novel photophysical, photochemical, redox and coordination properties. A particularly attractive feature of Pcs is the dependence of properties of the molecule on the nature of the peripheral functional groups, as well as the electronic properties of the central metal cations in the phthalocyanine ring [11]. Unsubstituted phthalocyanines are not very soluble and tend to aggregate in solution which results in the fast decay of the excited states. While the solubility can be increased by addition of alkoxy groups to peripheral positions or introducing of axial coordination groups to the central metal, tetrasubstituted phthalocyanines are usually more soluble than the corresponding octa-substituted due to the formation of isomers and the high dipole moment that results from the unsymmetrical arrangement of the substituents at the periphery [12].

In the fields of sustainable energy production, solar power technologies are emerging as one of the most promising alternatives. Developing efficient and affordable systems, able to harvest, convert, and store sunlight, are considered a very desirable approach toward obtaining clean energy [13]. A large number of Pcs as photosensitizer has been reported [14,15]. Meanwhile a good photosensitizer is required to be in its monomeric state for successful photo-induced energy and electron transfer [16]. So it is imperative to synthesis novel phthalocyanine to avoid aggregation and remain monomer.

Coumarins are fluorescent compounds that have interesting photophysical properties. They are excellent organic dye sensitizer because of strong absorption in visible zone [17]. The fluorescence quantum yield (Φ_F) of these dyes is usually very high, often close to unity [18]. Materials containing a coumarin component are useful in many fields due to their characteristics of high emission yield, excellent photostability and extended spectral range, such as fluorescence images [19]. The ground and excited state,

* Corresponding author. Tel.: +86 22 27404208; fax: +86 22 27892279.
E-mail address: wangshirong@tju.edu.cn (S.-R. Wang).

0143-7208/$ – see front matter
doi:10.1016/j.dyepig.2011.10.006

photophysical properties of 7-hydroxy-4-methylcoumarin have been intensively investigated [20].

To the best of our knowledge, 7-hydroxy-4-methylcoumarin tetrasubstituted ruthenium, indium and tin chloro phthalocyanines have not been reported. Herein we report the synthesis, fluorescence and thermal properties of 7-hydroxy-4-methylcoumarin tetrasubstituted metallophthalocyanines with axial chloride ligand.

2. Experimental

2.1. Materials

All solvents were reagent-grade quality and were obtained from commercial suppliers. All of them were dried and purified as described by Perin and Armarego [21]. Ruthenium(III) chloride, indium(III) chloride, tin(II) chloride, K_2CO_3, 1,5-diazabicyclo[4.3.0] non-5-ene(DBU), deuterated $CDCl_3$ and DMSO, were purchased from commercial suppliers too.

2.2. Measurements

Infrared spectra in KBr pellets were recorded on BIO-RAD FIS3000 spectrophotometer. UV–visible/NIR spectra were recorded on a Nicoet Evolution 300 spectrophotometer. ^{1}H NMR spectra were recorded with an INOVA 500MHz spectrometer. Mass spectra were recorded on a MALDI (Matrix Assisted Laser Desorption Ionization) Bruker Autoflex TOF (III) using 2,5-dihydroxybenzoic acid (DHB) as matrix. Element Analyses were carried out on a Vario Micro cube Analyzer. XPS spectra were recorded using a Kratos Axis Ultra DLD spectrometer employing a monochromated Al–Ka X-ray source (hv = 1486.6 eV), hybrid (magnetic/electrostatic) optics and a multi-channel plate and delay line detector (DLD). All XPS spectra were recorded using an aperture slot of 300*700 microns, survey spectra were recorded with a pass energy of 80 eV, and high resolution spectra with a pass energy of 40 eV. In order to subtract the surface charging effect, the C1s peak has been fixed at a binding energy of 284.6 eV. Fluorescence excitation and emission spectra were recorded on a Varian Cary Eclipse spectrofluorometer. Fluorescence lifetimes were measured using a time correlated single photon counting setup (TCSPC) (FluoroLog3, HORIBA Jobin Yvon) with a NanoLED-460 laser as excitation source (HORIBA Jobin Yvon). The optical filter in front of the detector was 630 nm to leach the light below it. And the peak present was 10,000, channels were 1024. All luminescence decay curves were measured at the maximum of emission peak. The data were analyzed with the program FluoroLog3 (HORIBA Jobin Yvon). The support plane approach [22] was used to estimate the errors of the decay times. Thermo gravimetric analyses were recorded on a Q500 Thermo gravimetric analyzer.

2.3. Fluorescence behavior

DMF and other solvents were dried and freshly distilled before use. Measurements were carried out at room temperature of 20 °C.

2.3.1. Fluorescence quantum yields

Fluorescence quantum yields (Φ_F) were determined by the comparative method (Equation (1)) [23,24].

$$\Phi_F = \Phi_{F(\mathrm{std})}\frac{F \cdot A_{\mathrm{std}} \cdot n^2}{F_{\mathrm{std}} \cdot A \cdot n^2_{\mathrm{std}}} \tag{1}$$

Where F and F_{std} are the areas under the florescence emission curves of the metallophthalocyanines (**4a**, **4b** and **4c**) and the standard, respectively. A and A_{std} are the relative absorbance of the sample and standard at the excitation wavelength, respectively. n and n_{std} are the refractive indices of solvents used for the sample and standard, respectively. Unsubstituted ZnPc (in DMSO) ($\Phi_F = 0.20$) [25] was employed as the standard. Both the sample and the standard were excited at the same relevant wavelength.

2.3.2. Fluorescence quenching by 1,4-benzoquine(BQ)

Fluorescence quenching experiments of **4a**, **4b** and **4c** were carried out by addition of different concentrations of the BQ to a fixed concentration of the complexes, and the concentrations of the BQ in the resulting mixtures were 0, 0.008, 0.016, 0.024, 0.032 and 0.040 M. The Fluorescence spectra of substituted metallophthalocyanines (**4a**, **4b** and **4c**) at each BQ concentration were recorded, and the changes in Fluorescence intensity related to BQ concentration by the Stern–Volmer (S–V) equation [26] were shown in Eq. (2)

$$\frac{I_0}{I} = 1 + K_{SV}[\mathrm{BQ}] \tag{2}$$

Where I_0 and I are the maximal fluorescence intensities of the fluorophore in the absence and presence of quencher, respectively. [BQ] is the concentration of the quencher. K_{SV} is the Stern–Volmer rate constant obtained from the slop. As shown in Eq. (3) k_q is the bimolecular quenching rate constant ($M^{-1} \bullet S^{-1}$) and τ_F is the main excited singlet lifetime of fluorophore (τ_1) in the absence of the quencher.

$$K_{SV} = K_q \cdot \tau_F \tag{3}$$

2.4. Synthesis

7-hydroxy-4-methylcoumarin(**1**) [27], 4-Nitrophthalonitrile(**2**) [28] was prepared according to the literature.

2.4.1. Synthesis of 7-(3,4-dicyanophenoxy)-4-methylcoumarin (3)

7-hydroxy-4-methylcoumarin (1.232 g, 7 mmol) and 4-nitrophthalonitrile (0.865 g, 5 mmol) was dissolved in dry DMF 40 ml. After 20 min stirring, finely ground anhydrous K_2CO_3 (1.035 g, 7.5 mmmol) was added portionwise over 2 h. And ensuring the mixture was stirred vigorously at room temperature till all 4-nitrophthalonitrile disappeared. Then the reaction mixture was poured into cold water (100 ml) to give the precipitate. After filtered, the solid was purified by silica gel column chromatography using ethyl acetate and cyclohexane as eluent. The product was soluble in acetone, ethyl acetate, tetrahydrofuran, chloroform, dichloromethane, dimethylformamide and dimethylsulfoxide. Yield: 0.962g, 63.7%, m.p. 228–230°C; IR ν_{max}/cm^{-1} (KBr pellet): 3073 (CH_{ar}), 2920–2855 (CH_{alkyl}), 2230 (C≡N), 1735(C=O), 1622(C=C), 1261 (Ar–O–Ar′); ^{1}H NMR (DMSO) δppm: 8.15 (d, 1H, Ar–H), 7.95 (d, 1H, Ar–H), 7.89 (d, 1H, Ar–H), 7.58 (q, 1H, Ar–H), 7.29 (d, 1H, Ar–H), 7.21 (q, 1H, Ar–H), 6.40 (s, 1H, C=CH), 2.46(s, 3H, CH_3).

2.4.2. Synthesis of 2,9,16,23-tetrakis(7-coumarinoxy-4-methyl)-phthalocyaninatoruthenium(*4a*)

A mixture of $RuCl_3 \bullet 3H_2O$ (0.209g, 0.8 mmol), 7-(3,4-dicyanophenoxy)-4-methylcoumarin (0.906 g, 3 mmol), DBU (10 drops) and octanol 40 ml were stirred and refluxed for 36 h under a nitrogen atmosphere. After cooling, the solution was dropped into petroleum to give greenish precipitate. The solid was washed with water to remove unreacted $RuCl_3 \bullet 3H_2O$. And then it was extracted by methanol till colorless. At last the crude product was dissolved in dichloromethane. After filtering and concentrating, the green product was purified by silica gel column chromatography using

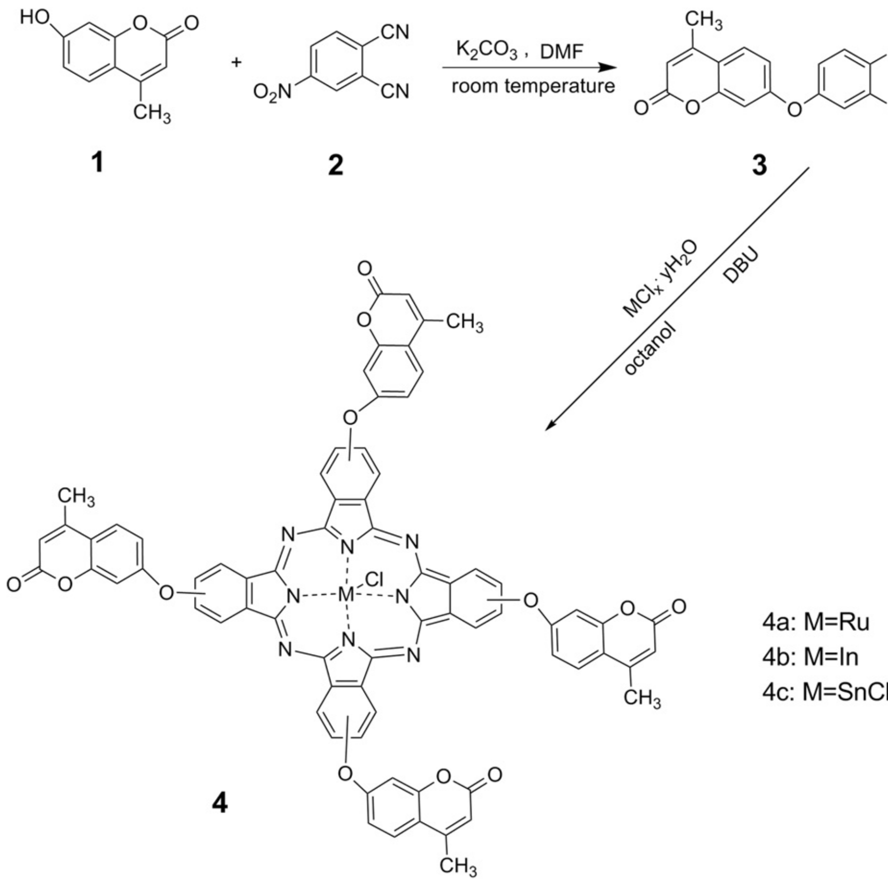

Scheme 1. Synthesis of 7-hydroxy-4-methylcoumarin tetrasubsitituted metallophthalocyanines complexes.

dichloromethane and ethanol as eluent. The product was soluble in acetone, tetrahydrofurane, chloroform, dichloromethane, dimethylformamide and dimethylsulfoxide. Yield: 0.250 g, 24.8%; m.p.: >300 OC; IR ν_{max}/cm^{-1} (KBr pellet): 3061 (CH_{ar}), 2919–2854 (CH_{alkyl}), 1732(C=O), 1602(C=C), 1273(Ar–O–Ar′); ^{1}H NMR (DMSO) δppm: 9.24–9.33 (m, 4H, Pc-H), 8.85–8.93 (m, 4H, Ar–H), 7.85–7.95 (m, 4H, Ar–H), 7.18–7.42 (m, 8H, Pc–H), 7.05–7.08 (m, 4H, Ar–H), 6.36 (s, 4H, C=CH), 2.50 (s, 12H, CH_3); MS(MALDI–TOF) *m*/*z*: Calc.1345; Found: 1310 [M – Cl]$^+$; Anal. Calc. for $C_{72}H_{40}N_8O_{12}ClRu$: C, 64.26; H, 3.00; N, 8.33; Found: C, 64.31; H, 2.95; N, 8.25.

2.4.3. Synthesis of 2,9,16,23-tetrakis(7-coumarinoxy-4-methyl)-phthalocyaninatoindium (4b)

Compound **4b** was prepared and purified according to the procedure described for **4a**, starting from $InCl_3{\bullet}4H_2O$ (0.234 g, 0.8 mmol), 7-(3,4-dicyanophenoxy)-4-methylcoumarin (0.906 g, 3 mmol), DBU (10 drops) and octanol 40 ml. Yield: 0.589 g, 57.8%; m.p.: >300 OC; IR ν_{max}/cm^{-1} (KBr pellet): 3064 (CH_{ar}), 2921–2851(CH_{alkyl}), 1717(C=O), 1605(C=C), 1271(Ar–O–Ar′); ^{1}H NMR ($CDCl_3$) δppm: 9.03–9.11 (m, 4H, Pc–H), 8.68–8.72 (m, 4H, Ar–H), 7.83–7.86(m, 4H, Ar–H), 7.58–7.72 (m, 8H, Pc–H), 7.34–7.29 (m, 4H, Ar–H), 6.24 (s, 4H, C=CH), 2.49 (s, 12H, CH_3); MS(MALDI–TOF) *m*/*z*: Calc. *m*/*z*: Calc.1358; Found:1323 [M – Cl]$^+$; Anal. Calc. for $C_{72}H_{40}N_8O_{12}ClIn$: C, 63.61; H, 2.97; N, 8.24; Found: C, 63.55; H, 2.93; N, 8.12.

2.4.4. Synthesis of 2,9,16,23-tetrakis(7-coumarinoxy-4-methyl)-phthalocyaninatotin (4c)

Compound **4c** was prepared and purified according to the procedure described for **4a**, starting from $SnCl_2{\bullet}2H_2O$ (0.180 g, 0.8 mmol), 7-(3,4-dicyanophenoxy)-4-methylcoumarin (0.906 g, 3 mmol), DBU (10 drops) and octanol 40 ml. Yield: 0.241 g, 23.1%; m.p.: >300 OC; IR ν_{max}/cm^{-1} (KBr pellet): 3065 (CH_{ar}), 2931–2846 (CH_{alkyl}), 1729(C=O), 1601(C=C), 1265(Ar–O–Ar′); ^{1}H NMR ($CDCl_3$) δppm: 9.55–9.66 (m, 4H, Pc–H), 9.16–9.22 (m, 4H, Ar–H), 8.02–8.12 (m, 4H, Ar–H), 7.50–7.77 (m, 8H, Pc–H), 7.36–7.38 (m, 4H, Ar–H), 6.30 (s, 4H, C=CH), 2.50 (s, 12H, CH_3); MS(MALDI–TOF) *m*/*z*: Calc. 1398; Found: 1363 [M – Cl]$^+$, 1328 [M – 2Cl]$^+$; Anal. Calc. for $C_{72}H_{40}N_8O_{12}Cl_2Sn$: C, 61.82; H, 2.88; N, 8.01; Found: C, 61.73; H, 2.96; N, 7.97.

3. Results and discussion

3.1. Synthesis and characterization

The route for the synthesis of 2,9,16,23-tetrakis(7-coumarinoxy-4-methyl)-metallophthalocyanines **4a, 4b, 4c** is given in Scheme 1. 7-(3,4-dicyanophenoxy)-4-methylcoumarin **3** was prepared by a base catalyzed nucleophilic aromatic nitro displacement of 7-hydroxy-4-methylcoumarin **1** with 4-nitrophthalonitrile **2** according to the published procedures [29]. The reaction was carried out by using K_2CO_3 as the nitro-displacing base at room temperature in dried dimethylformamide as the solvent. Therefore cyclotetramerization of 7-(3,4-dicyanophenoxy)-4-methylcoumarin **3** in the presence of $RuCl_3{\bullet}3H_2O$, $InCl_3{\bullet}4H_2O$ or $SnCl_2{\bullet}2H_2O$ and DBU in octanol gave the 2,9,16,23-tetrakis (7-coumarinoxy-4-methyl) substituted Ruthenium, Indium or Tin phthalocyanine derivatives respectively.

Spectral data of the newly synthesized compounds are consistent with the proposed structures. Comparison of the IR spectral data clearly indicated the formation of compound **3**. The new bands

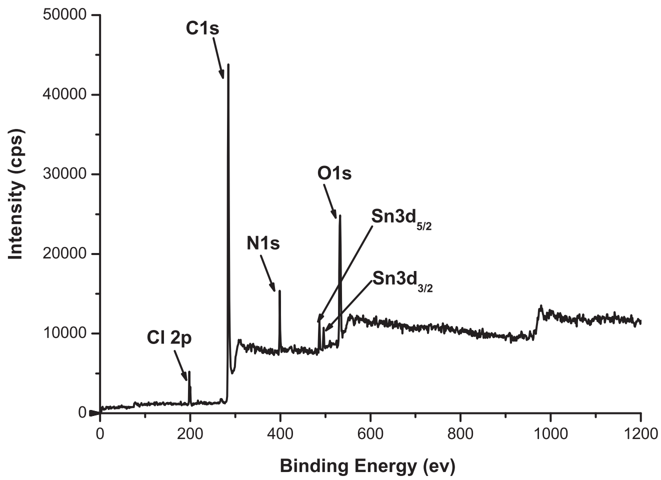

Fig. 1. XPS spectrum of **4c**.

of Ar–O–Ar at 1265 cm^{-1} and disappearance of the –OH and –NO_2 bands at 3500 cm^{-1} and 1536–1349 cm^{-1} prove the compound **3** was formed. All the complexes show peaks between 1000 and 700 cm^{-1} which may be assigned to phthalocyanines skeletal vibrations [30]. The complexes show characteristic vibrations due to aromatic CH stretching at ca. 3061–3065 cm^{-1},carbonyl C = O stretching at ca. 1717–1732 cm^{-1} and ether group (C–O–C) at 1261–1273 cm^{-1}.

The ^{1}H NMR spectra of phthalocyanines **4a**–**4c** are almost identical. The expected signals are observed in accordance with the proposed phthalocyanine structures [31]. Both complex types are expected to have isomers due to the presence of a substituent on either peripheral position. **4a** shows two sets of multiplets at 9.24–9.33 and 7.85–7.95 ppm for the phthalocyanine ring, integrating for 12 protons. The aromatic protons are observed as multiplets at 8.85–8.93, 7.85–7.95, 7.05–7.08 ppm integrating 12 protons. Unsaturated and methyl protons are appeared at 6.36 ppm (4 protons) and 2.50 ppm (12 protons) as singlets. **4b** also give similar signals with 2 sets of multiplets for Pc ring at 9.03–9.11, 7.58–7.72 ppm and 12 protons for aryl protons at 8.68–8.72, 7.83–7.86, 7.29–7.34 ppm respectively. And 4 unsaturated protons at 6.24 ppm and 12 methyl protons at 2.49 ppm as signets are found too. The ^{1}H NMR of **4c** shows similar spectral figures as **4a, 4b** with

Table 1
Fluorescence and UV–visible spectral properties of **4a**, **4b**, **4c** in DMF.

Compound	Q-band wavelength (nm)	Excitation wavelength (nm)	Emission wavelength (nm)	Stokes shift (nm)	Fluorescene quantum yield (Φ_F)
4a	650	677	694	17	0.005
4b	693	687	697	10	0.016
4c	678	703	704	1	0.009

the three sets of aromatic protons at 9.16–9.22, 8.02–8.12, 7.36–7.38 ppm as multiplets. The spectrum also gives two sets of Pc rings at 9.55–9.66, 7.50–7.77 ppm as multiplets means 12 protons too. The unsaturated protons at 6.30 ppm and methyl protons at 2.50 ppm as signets indicate each 4 protons at the same time. The mass spectra which were obtained by MALDI–TOF (2,5-dihydroxybenzoic acid was used as matrix) were consistent with assigned formulations without chlorine atoms [32].

Survey XPS scans show the presence of C, O, N, Cl and the corresponding metal with no other elements being observed [33,34,35]. Fig. 1. shows the XPS spectrum of **4c** as an example: C 1s (284.6 eV), O 1s (531.9 eV), N 1s (398.5 eV). The XPS Cl 2p spectrum consists of $2p_{3/2}$ and $2p_{1/2}$ with the intensity ratio 2:1. The components are located at 198.3 and 200.0 eV that corresponds to the M–Cl bonding [33,35]. The binding energy of the Sn $3d_{5/2}$ level is measured to be 487.1 eV and the $3d_{3/2}$ is 495.5 eV. Other than the identical N 1s, O 1s, C 1s and Cl 2p peaks, the XPS spectra for **4a** and **4b** show Ru $3d_{5/2}$ and In $3d_{5/2}$ peaks at 281.1 and 444.91 eV, respectively. Most importantly the XPS determined N:Metal:Cl ratio are 8:1:1, 8:1:1 and 8:1:2 for **4a, 4b** and **4c** in excellent agreement with the stoichiometry of the complexes.

3.2. Ground state electronic absorption

The ground state electronic absorption spectra (Fig. 2.) show monomeric behavior evidence by a single Q-band, typical of metallophthalocyanine complexes [36].

The π–π^* Soret transition toward the second singlet excited state is observed at around 320 nm. The shoulder between 400 and 460 nm may due to a charge transfer from the electron-rich phthalocyanine ring to the electron-poor central metal. The Q-bands are seen in the near infrared region 600–720 nm. It is

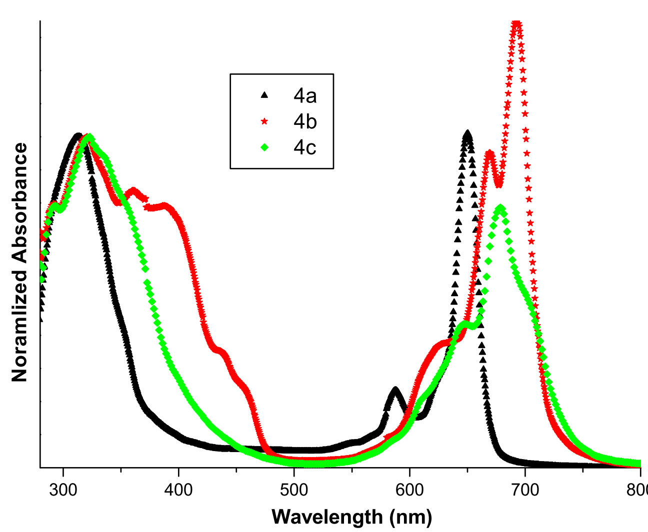

Fig. 2. Ground state electronic absorption spectra of **4a**, **4b**, **4c** in DMF.

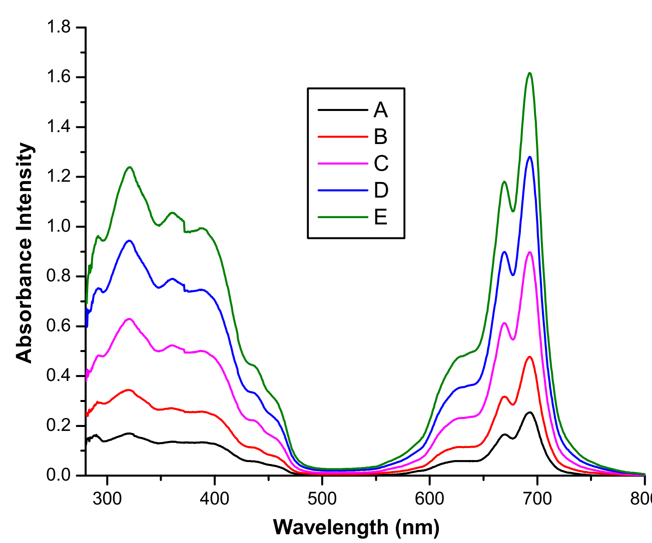

Fig. 3. Aggregation behavior of **4b** in DMF at different concentrations: (A) 2.5 × 10^{-6}, (B) 5 × 10^{-6}, (C) 10 × 10^{-6}, (D) 15 × 10^{-6} and (E) 20 × 10^{-6} M.

reported, for phthalocyanines, loss of symmetry will result in splitting of spectra [37]. All of the three metallophthalocyanines in our research show splitting Q-bands for that Ru, In and Sn are larger metal not fitting into the Pc ring.

The Q-band absorption maxima in DMF of the three metallophthalocyanines are observed at different wavelength. As shown in Table 1, **4b** (Q-band at 693 nm) and **4c** (Q-band at 678 nm) are bathochromic-shifted relative to **4a** (Q-band at 650 nm) which agrees with the electronegativity of the central metal.

Aggregation is usually depicted as a coplanar association of rings progressing from monomer to dimmer and higher order complexes. It is dependent on the concentration, nature of the solvent, nature of the substituents, complexed metalions and temperature [38]. In this study, the aggregation behavior of 7-hydroxy-4-methylcoumarin tetrasubstituted metallophthalocyanines (**4a**–**4c**) was investigated at different concentrations in DMF (Fig. 3. for complex **4b** as an example). As the concentration was increased, the intensity of the absorption of the Q-band maxima also increased and there were no new bands (normally blue shifted) due to the aggregated species for all the studied metallophthalocyanines (**4a**–**4c**). The Beer–Lambert law was obeyed for all of the three compounds at concentrations ranging from 2.5×10^{-6} to 2×10^{-5} M.

3.3. Fluorescence spectra and properties

Shown in Fig. 4, are the Q-bands absorption, fluorescence excitation and emission spectra of the metallophthalocyanines **4a**–**4c** in DMF. The shapes of excitation spectra were similar to the absorption spectra and are mirror images to the fluorescence emission spectra for all the phthalocyanines (**4a**–**4c**). Fluorescence emission peaks were observed at: 694 nm for **4a**, 697 nm for **4b** and 704 nm for **4c** in DMF. The fluorescence excitation and emission spectra of Complexes are typical of phthalocyanines, with Stokes' shifts ($\lambda_{Em} - \lambda_{Exci}$) ranging from 1 to 17 nm (Table 1). The Q-bands maxima of excitation and absorption spectra are different ($\Delta\lambda = \lambda_{Exci} - \lambda_{Q}$), especially for **4a** (27 nm) and **4c** (25 nm), suggesting a large structure change between the ground and excited states. These phenomena are attributed to the fact that Ru, In and Sn are metals with large atomic numbers that can be displaced

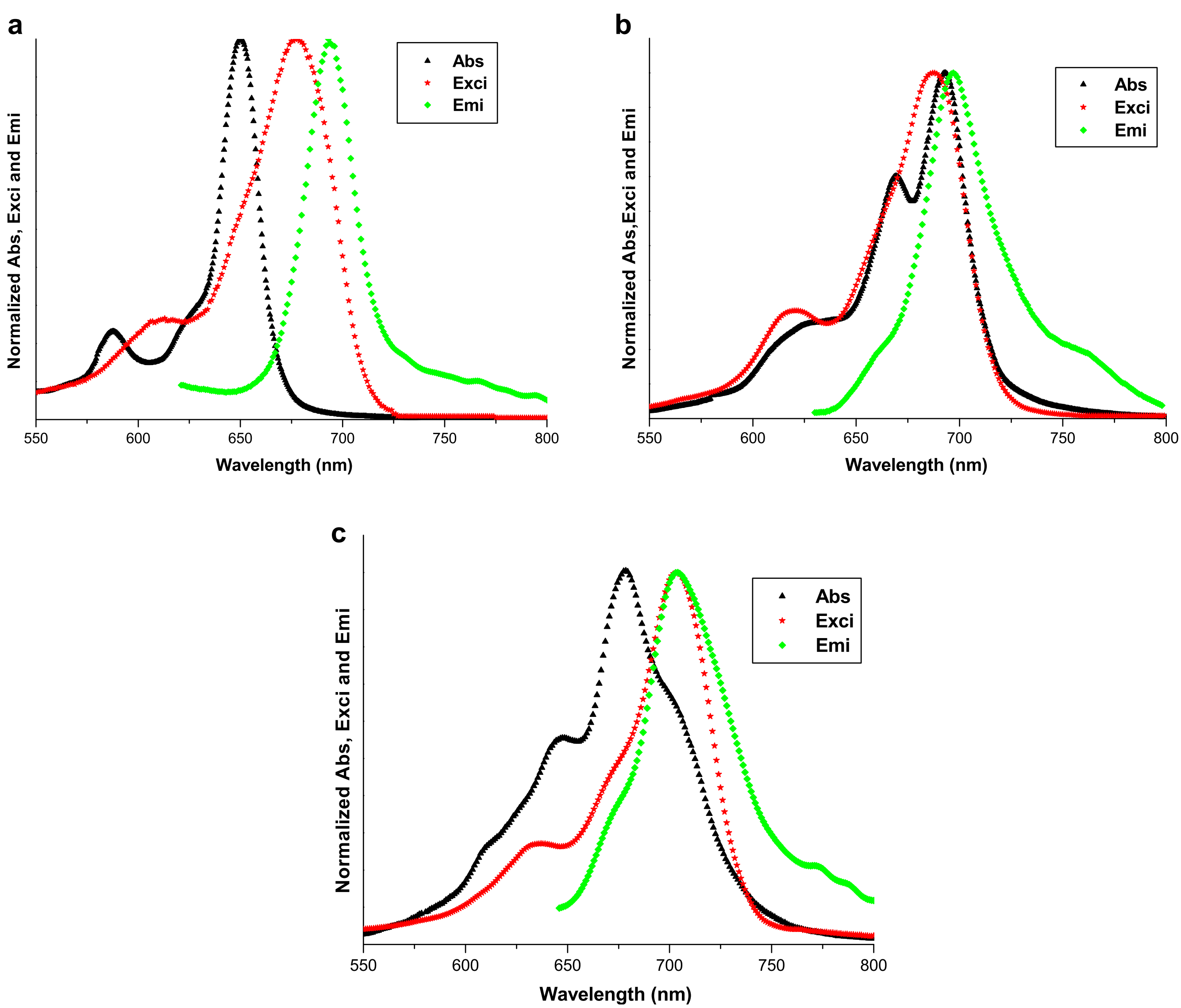

Fig. 4. UV–vis absorption (Abs), excitation (Exci) and fluorescene emission (Emi) spectra of compound **4a**, **4b**, **4c** in DMF. Excitation wavelengths: 610 nm for **4a**, 618 nm for **4b** and 635 nm for **4c**.

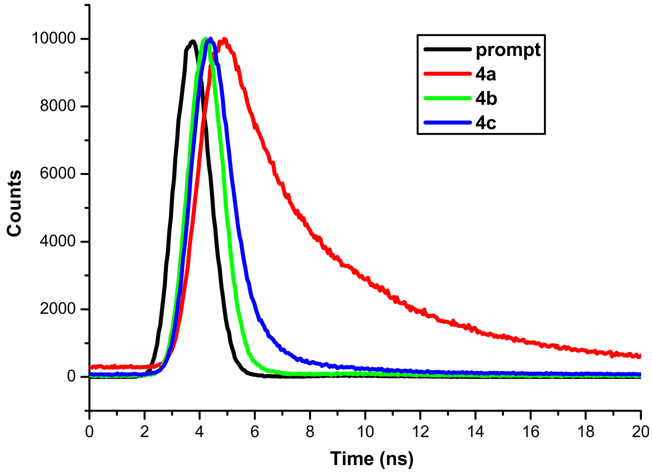

Fig. 5. Photoluminescence decay curve of **4a**, **4b**, **4c** in DMF.

Table 2
Fluorescence lifetime of **4a**, **4b**, **4c** in DMF.

Compound	τ_1/ns	α_1/%	τ_2/ns	α_2/%
4a	4.5	87.44	1.41	12.65
4b	0.09	97.70	1.84	2.30
4c	0.4	85.29	1.97	14.71

α normalized (to 100) fractional amplitude.

from the core of the Pc ring on excitation, hence resulting into a loss of symmetry [39].

3.4. Fluorescence quantum yields (Φ_F) and fluorescence lifetime (τ_F)

The fluorescence quantum yields (Φ_F) of compounds **4a, 4b, 4c** are given in Table 1. The Φ_F values are found be less than 0.1 due to the presence the heavy atom (Ru, In, and Sn). The values of Φ_F vary much upon the central metals. Because of different spin–orbit coupling for different metals, the heavier the central metal is, the stronger the spin–orbital coupling and the shorter the energy gap between S1 and T1 states, and therefore the more probability of intersystem crossing from S1 to T1 states, which results in low quantity of Φ_F [6,40]. Both **4b** and **4c** are close shell MPcs, the heavier metal Sn enhances more intersystem crossing (through spin orbit coupling), then afford lower Φ_F. The lowest fluorescence quantum yield observed for **4a** is due to the open-shell nature of the metal which promotes d–π interactions thereby quenching the singlet state of the complexes. Also the enhanced spin orbit coupling might be responsible for the lowering of fluorescence quantum yields [41].

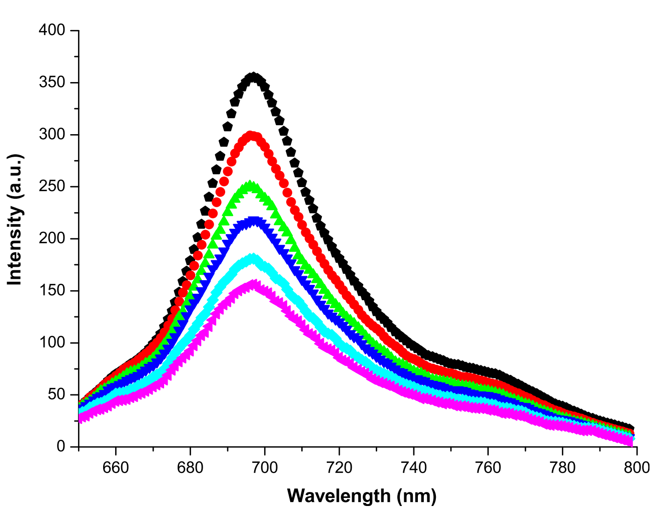

Fig. 6. Fluorescence emission spectral changes of **4b** (1.00×10^{-5} M) on addition of different concentrations of BQ in toluene. [BQ] = 0, 0.008, 0.016, 0.024, 0.032, 0.040 M.

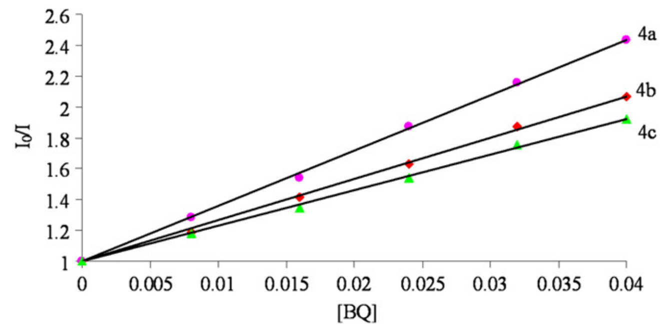

Fig. 7. Sterne–Volmer plots for benzoquinone (BQ) quenching of **4a**, **4b**, **4c**. [MPc]: 1.00×10^{-5} M in DMF. [BQ] = 0, 0.008, 0.016, 0.024, 0.032, 0.040 M.

Table 3
Fluorescence quenching data for **4a**, **4b**, **4c** in DMF.

Compound	K_{SV} (M^{-1})	$k_q/10^{10}$ (M^{-1} S^{-1})
4a	35.86	0.8
4b	26.61	29.6
4c	22.99	5.75

Fig. 5 shows the time-resolved fluorescence decay curve for **4a**, **4b** and **4c** in DMF, indicating a biexponential decay. Fluorescence lifetime (τ_F) refers to the average time a molecule stays in its excited state before fluorescing. The nature and the environment of a fluorophore determine its fluorescence lifetime. Shown in Table 2, are the two kinds of lifetime of metallophthalocyanines **4a**–**4c** of S1 state. The shorter lifetime τ_1 of **4b** and **4c** is due to the intersystem crossing processing to the triplet state enhanced by In and Sn atom [6]. The lifetime of **4a** is extraordinarylonger than **4b** and **4c** for the nature of Ru metal. **4a**, **4b** and **4c** have a similar lifetime of τ_2. This emission of the photoproduct is due to the photo-induced metal ejection process. It is as a result of photoexcitation, the metal ion changes its position in a vertical direction with respect to the plane of phthalocyanine macrocycle. If the metal does not return quickly (on S1 surface) to its chelating ring an emission characteristic for metal-free phthalocyanine could be recorded [39,42,43]. The elemental analysis of the samples can not show the presence of such impurity at the S_0 state. In our study, Both **4a** and **4c** show larger $\Delta\lambda$ ($\lambda_{Exci} - \lambda_Q$) so the proportion of τ_2 is more than that of **4b**. While the amplitude of τ_2 is significantly smaller than that of τ_1 indicating τ_1 is the main decay of the three compounds.

Table 4
Thermal properties of **4a**, **4b**, **4c**.

Compound	T5% (°C)[a]	D (°C)[b]	Yc (%)[c]
4a	322	400	65.3
4b	370	450	65.2
4c	175	191	59.4

[a] The temperature for which the weight loss is 5%.
[b] The temperature for which the compound is decomposed.
[c] Char yield at 600 OC.

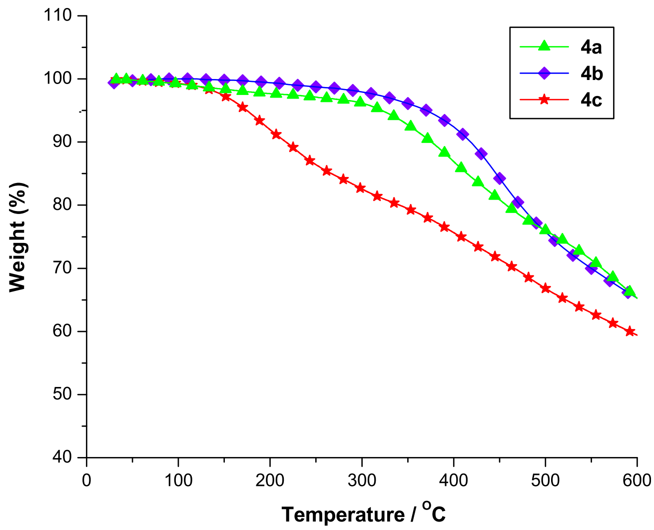

Fig. 8. The TGA profile of **4a**, **4b**, **4c**.

3.5. Fluorescence quenching studies by 1,4-benzoquinone [BQ]

The fluorescence quenching of substituted phthalocyanine complexes (**4a**, **4b**, **4c**) by BQ in different concentration is found to obey Stern–Volmer kinetics. An essential requirement for good light harvesting materials is the ability to undergo excited state charge transfer with ease. The energy of the lowest excited state for quinones is greater than the energy of the excited singlet state of MPc complexes [44]. Therefore metallophthalocyanine fluorescence quenching by BQ is via excited state electron transfer, from the metallophthalocyanine to the BQ [45]. It is observed that fluorescence spectrum when taken with increasing concentration of BQ does not show any shift in wavelength. There is no additional peak appearing; hence there could not be any ground-state interaction between MPcs and BQ. Fig. 6 shows the quenching of **4b** complex by BQ in DMF as an example. K_{SV} values are given by the slope of the plots shown at Fig. 7. The Stern–Volmer plots for all studied complexes (**4a**, **4b**, **4c**) give straight lines, depicting diffusion-controlled quenching mechanisms. The K_{SV} and bimolecular quenching constant (k_q) values for the BQ quenching of phthalocyanine complexes are shown in Table 3. **4b** shows the highest k_q of 29.6×10^{10} M^{-1} S^{-1}, and **4a** shows the lowest k_q of 0.8×10^{10} M^{-1} S^{-1} which is in accordance with fluorescence quantum yields (Φ_F). The k_q values are found to be close to the diffusion-controlled limits, $\sim 10^{10}$ M^{-1} s^{-1}, which is in agreement with the Einstein–Smoluchowski approximation at room temperature for diffusion-controlled bimolecular interactions [46].

3.6. Thermal properties

The thermal stability of the Pcs was tested by the TGA analysis (Fig. 8), and the results are summarized in Table 4. The samples were heated from 30 to 600 °C in a nitrogen flow with a heating rate of 10 °C min^{-1}. There is a 5% weight loss at 322 °C, 370 °C and 175 °C, for **4a, 4b** and **4c**, respectively. It is due to the loss of physically absorbed water. Further decomposition is observed for all metallophthalocyanines. The loss of chlorine occurs at 400 °C, 450 °C and 191 °C for **4a, 4b** and **4c**, respectively, indicating that **4a** and **4b** have higher thermal stability than **4c**.

4. Conclusions

In the present work, we have successfully synthesized three novel 7-hydroxy-4-methylcoumarin tetrasubstituted metallophthalocyanines with axial chloride ligand (**4a, 4b, 4c**). All of the three phthalocyanines show excellent solubility in various solvents such as acetone, tetrahydrofurane, chloroform, dichloromethane, dimethylformamide and dimethylsulfoxide. In the ground state absorption all of the three metallophthalocyanines show splitting Q-bands for that Ru, In and Sn are large metals not fitting into the Pc ring. The open-shell metallophthalocyanine (**4a**) shows the lowest fluorescence quantum yields for d–π interactions and spin orbital coupling effect; while it appears the highest fluorescence lifetime owing to the relatively lower atomic number.

The order of fluorescence quantum yields is **4b** > **4c** > **4a** and the main fluorescence lifetime (τ_1) is **4a** >**4c** > **4b**. This work also presents the light harvesting and energy transducing tendencies of the mixtures of metallophthalocyanine complexes with BQ. **4b** shows the highest k_q value and **4a** shows the lowest which is in accordance with fluorescence quantum yields (Φ_F). All of the three metallophthalocyanines could serve as good light harvesters and energy transducers. Both **4a** and **4b** show high thermal stability than **4c**.

Acknowledgments

This work was financially supported by Natural Science Foundation of Tianjin China (08JCZDJC16900), Natural Science Foundation of China (NSFC 21176180) and Research Fund for the Doctoral Program of Higher Education of China (20100032110021).

References

[1] Simon J, Bassoul P. Design of molecular materials: supramolecular engineering. Weinheim: VCH; 2000.
[2] Detty M, Gibson SL, Wagner SJ. Current clinical and preclinical photosensitizer for use in photodynamic therapy. J Med Chem 2004;47:3897–915.
[3] Durmus M, Ahsen V. Water-soluble cationic gallium(III) and indium(III) phthalocyanines for photodynamic therapy. J Inorg Biochem 2010;104: 297–309.
[4] Zeng Y, Wang XL, Yang YJ, Chen JF, Fu JW, Tao X. Assembling photosensitive capsules by phthalocyanines and polyelectrolytes for photodynamic therapy. Polymer 2011;52:1766–71.
[5] Yu SK, Ma CY, Cheng CH, Wang X, Ji DM, Fan ZQ, et al. Synthesis and 0.88 μm near-infrared electroluminescence properties of a soluble choloroindium phthalocynaine. Dyes Pigm 2008;76:492–8.
[6] Snow A, Bager WR. Phthalocynaines film in chemical sensors. In: Leznoff CC, Lever ABP, editors. Phthalocyanines-properties and applications, vol. 1. New York: VCH; 1989. p. 341–92.
[7] Pereira AMVM, Soares ARM, Calvete MJF, Gema DLTe. Recent developments in the synthesis of homo- and heteroarrays of porphyrins and phthalocyanines. J Porphyr Phthalocyanines 2009;13:419–28.
[8] Chen XC, Thomas J, Gangopadhyay P, Norwood RA, Peyghambarian N, McGrath D. Modification of symmetrically substituted phthalocyanines using click chemistry: phthalocyanine nanostructures by nanoimprint lithography. J Am Chem Soc 2009;131:13840–3.
[9] Wang XY, Zhang YX, Sun X, Bian YZ, Ma CQ, Jiang JZ. 2,3,9,10,16,17,24,25-Octakis(octyloxycarbonyl)phthalocyanines, synthesis, spectroscopic, and electrochemical characteristics. Inorg Chem 2007;46:7136–41.
[10] Rawling T, Austin C, Buchholz F, Colbran SB. Ruthenium phthalocyanine–bipyridyl dyads as sensitizers for dye-sensitized solar cells: dye coverage versus molecular efficiency. Inorg Chem 2009;48:3215–27.
[11] Osburn EJ, Chau LK, Chen SY, Collins N, Obrien DF, Armstrong NR. Novel amphiphilic phthalocyanines: formation of Langmuir–Blodgett and cast thin films. Langmuir 1996;12:4784–96.
[12] Beck A, Mangold KM, Hanack M. Lösliche (tetraethylphthalocyaninato)eisen(II)- und -cobalt(II)-Verbindungen. Chem Ber 1991;124:2315–21.
[13] Collings A, Critchley C. Artificial photosynthesis: from basic biology to industrial application. Germany: Wiley-VCH Verlag GmbH & Co; 2005. KGaA: Weinheim.
[14] Morandeira A, Lopez-Duarte I, Martinez-Diaz MV, O'Regan B, Shuttle C, Haji-Zainulabidin NA, et al. Slow electron injection on Ru–phthalocyanine sensitized TiO_2. J Am Chem Soc 2007;129:9250–1.
[15] Cid JJ, Yum JH, Jang SR, Nazeeruddin MK, Martínez-Ferrero E, Palomares E, et al. Molecular cosensitization for efficient panchromatic dye-sensitized solar cells. Angew Chem Int Ed 2007;46:8358–62.

[16] Harriman A, Richoux MC. Attempted photoproduction of hydrogen using sulphophthalocyanines as chromophores for three-component systems. J Chem Soc Faraday Trans 1980;76:1618–26.
[17] Wang Z-S, Cui Y, Hara K, Dan-oh Y, Kasada C, Shinpo A. A high-light-harvesting-efficiency coumarin dye for stable dye-sensitized solar cells. Adv Mater 2007;19:1138–41.
[18] Jones G, Jackson WR, Choi CY, Bergmark WR. Solvent effects on emission yield and lifetime for coumarin laser dyes. Requirements for a rotatory decay mechanism. J Phys Chem 1985;89:294–300.
[19] Wang BY, Liu XY, Hu YL, Su ZX. Synthesis and photophysical behavior of a water-soluble coumarin-bearing polymer for proton and Ni^{2+} ion sensing. Polym Int 2009;58:703–9.
[20] Setsukinai K, Urano Y, Kikuchi K, Higuchi T, Nagano T. Fluorescence switching by O-dearylation of 7-aryloxycoumarins. Development of novel fluorescence probes to detect reactive oxygen species with high selectivity. J Chem Soc Perkin Trans 2000;2:2453–7.
[21] Perin DD, Armarego WLF. Purification of laboratory chemicals. 2nd ed. New York: Pergamon Press; 1985.
[22] Lakowicz JR. Principles of fluorescence spectroscopy. 3rd ed. New York: Kluwer Academic/Pleum Publishers; 1999. 97–122.
[23] Maree D, Nyokong T, Suhling K, Phillips D. Effects of axial ligands on the photophysical properties of silicon octaphenoxyphthalocyanine. J Porphyr Phthalocyanines 2002;6:373–6.
[24] Fery-Forgues S, Lavabre D. Are fluorescence quantum yields so tricky to measure? A demonstration using familiar stationery products. J Chem Educ 1999;76:1260–4.
[25] Ogunsipe A, Chen JY, Nyokong T. Photophysical and photochemical studies of zinc(II) phthalocyanine derivatives-effects of substituents and solvents. New J Chem 2004;28:822–7.
[26] Rose J. Advanced physico-chemical experiments. London: Sir Isaac Pitman & Sons Ltd; 1964.
[27] Hiroki M, Kubo K, Tadamitsu S, Hiroyasu I. Solvent effects on the proton-transfer reactions of 7-hydroxycoumarin and its 4-methyl derivative with tertiary amines in the ground and excited singlet states. Ber Bunsenges Phys Chem 1997;101:1914–20.
[28] Acher BN, Fohlen GM, Parker JA, Keshavayya J. Synthesis and structure studies of metal (II) 2,9,14,23-phthalocyanine tetraamines. Polyhedron 1987;6:1463–7.
[29] Esenpinar AA, Bulut M. Synthesis and characterization of metal-free and metallo-phthalocyanines with four pendant coumarinthio/oxy-substituents. Dyes Pigm 2008;76:249–55.
[30] Sidorov AN, Terenin AN. Infrared spectra of phthalocyanines. II. Interaction of sublimed layers of phthalocyanines with gaseous CH_3COOH, HCl, and HBr. Opt Spectro 1961;11:175–8.
[31] Luo QF, Tian H, Chen BZ, Huang W. Effective non-destructive readout of photochromic bisthienylethene-phthalocyanine hybrid. Dyes Pigm 2007;73: 118–20.
[32] Yanki H, Aydin D, Durmus M, Ahsen V. Perpheral and non-perpheral tetrasubstituted aluminium, gallium and indium phthalocyanines: synthesis, photophysics and photochemistry. J Photochem Photobiol A 2009;26:18–26.
[33] Brant P, Stephenson TA. X-ray photoelectron spectra of mixed-valence diruthenium complexes. Distinguishing between strongly and weakly interacting metals in delocalized class 111 complexes. Inorg Chem 1987;26:22–6.
[34] Freeland BH, Habeeb JJ, Tuck DG. Coordination compounds of indium. Part XXXIII. X-ray photoelectron spectroscopy of neutral and anionic indium halide species. Can J Chem 1977;55:1527–32.
[35] Camalli M, Caruso F, Mattogno G, Rivarola E. Adducts of tin(IV) and organotin(IV) derivatives with 2,2′-azopyridine II. Crystal and molecular structure of $SnMe_2Br_2AZP$ and further mossbauer and photoelectronic spectroscopic studies. Inorg Chim Acta 1990;170:225–31.
[36] Stillman MJ, Nyokong T. Absorption and magnetic circular dichroism spectral properties of phthalocyanines. Part 1: complexes of the dianion, Pc(−2). In: Leznoff CC, Lever ABP, editors. Phthalocyanines: properties and applications, vol. 1. New York: VCH Publishers; 1989. p. 133–289.
[37] Masilela N, Nyokong T. The synthesis and photophysical properties of water soluble tetrasulfonated octacarboxylated and quaternised 2,(3)-tetra-(2-pyridiloxy)Ga phthalocyanines. Dyes Pigm 2010;84:242–8.
[38] Engelkamp H, Nolte RJM. Molecular materials based on crown ether functionalized phthalocyanines. J Porphyrins Phthalocyanines 2000;4:454–9.
[39] Durmus M, Nkokong T. Photophysical and photochemical properties of aryloxy tetra-substituted gallium and indium phthalocyanine derivatives. Tetrahedron 2007;63:1385–94.
[40] Chen J, Gan Q, Li SY, Gong FB, Wang Q, Yang ZP, et al. The effects of central metals and peripheral substituents on the photophysical properties and optical limting performance of phthalocyanines with axial chloride ligand. J Photoch Photobio A 2009;207:58–65.
[41] Senge MO. Exercises in molecular gymnastics—bending, stretching and twisting porphyrins. Chem Commun; 2006:243–56.
[42] Gao B, Yang Li, Jianhua Su, Tian H. Self-assembly of perylene bismide bridging ligands to zinc phthalocuanine in solution. Supramolecualr Chem 2007;19: 207–10.
[43] Synak A, Gil M, Organero JA, Marta FS, Douhal A. Iglesias fast to ultrafast dynamics of palladium phthalocyanine covalently bonded to MCM-41 mesoporous material. J Phys Chem C 2009;113:19199–207.
[44] Darwent JR, McCubbin I, Phillips DJ. Excited singlet and triplet state electron-transfer reactions of aluminium(III) sulphonated phthalocyanine. J Chem Soc Faraday Trans 1982;78:347–57.
[45] Idowu M, Nyokong T. Photophysicochemical and fluorescence quenching studies of tetra- and octa-carboxy substituted silicon and germanium phthalocyanines. J Photochem Photobiol A Chem 2009;204:63–8.
[46] Dutt GB, Periasamy N. Electron-transfer distance in intermolecular diffusion-limited reactions. J Chem Soc Faraday Trans 1991;87:3815–20.